Drug Design, Development and Therapy

Dovepress
open access to scientific and medical research

Open Access Full Text Article

ORIGINAL RESEARCH

Paeoniflorin improves cardiac function and decreases adverse postinfarction left ventricular remodeling in a rat model of acute myocardial infarction

This article was published in the following Dove Press journal:
Drug Design, Development and Therapy

Hengwen Chen*
Yan Dong*
Xuanhui He
Jun Li
Jie Wang

Guang'anmen Hospital, China Academy of Chinese Medical Sciences, Beijing, China

*These authors contributed equally to this work

Background: Paeoniflorin (PF) is the active component of *Paeonia lactiflora* Pall. or *Paeonia veitchii* Lynch. This study was, therefore, aimed to evaluate the improvement and mechanism of the PF on ventricular remodeling in rats with acute myocardial infarction (AMI).

Materials and methods: In this study, AMI model was established by ligating the anterior descending coronary artery in Wistar rats. After 4 weeks gavage of PF, the apparent signs and the left ventricle weight index of Wistar rats were observed. The left ventricular ejection fraction (LVEF) was evaluated by Doppler ultrasonography. Changes in cardiac morphology were observed by pathologic examination, and apoptosis was observed by the terminal deoxynucleotidyl transferase dUTP nick end labeling assay. In addition, enzyme-linked immunosorbent assay was used to detect the expression of tumor necrosis factor-α (TNF-α), interleukin-6 (IL-6) interleukin-10 (IL-10) and brain natriuretic peptide (BNP). Immunohistochemistry and Western blot method were applied to detect Caspase-3 and Caspase-9.

Results: Compared with the model control, the survival conditions of rats in all treatment groups were generally improved after PF treatment. LVEF was significantly increased, and both left ventricular end-diastolic inner diameter and left ventricular end-systolic inner diameter were significantly reduced. Moreover, pathologic examination showed that the myocardium degeneration of the rats treated with PF was decreased, including neater arrangement, more complete myofilament, more uniform gap and less interstitial collagen fibers. Furthermore, the mitochondrial structure of cardiomyocytes was significantly improved. The ultrastructure was clear, and the arrangement of myofilament was more regular. Also, the expression of Caspase-3 and Caspase-9 was inhibited, and apoptosis was obviously reduced in the PF treatment groups. BNP, TNF-α and IL-6 were also decreased and IL-10 was increased in the treated rats.

Conclusion: PF could significantly improve the LVEF of rats. It decreased adverse left ventricular remodeling after myocardial infarction in rat models. The potential mechanism could be that PF decreased and inhibited BNP, TNF-α and IL-6, increased IL-10 and further inhibited the expression of Caspase-3 and Caspase-9, thus promoting ventricular remodeling.

Keywords: paeoniflorin, ventricular remodeling, myocardial infarction, Caspase-3, Caspase-9

Introduction

Acute myocardial infarction (AMI) is caused by a sudden and severe decrease or interruption of blood supply in coronary artery processes, thus resulting in severe acute ischemia in the myocardium and further ischemic necrosis.[1] Ventricular remodeling (VR) is the change of the ventricular shape and structure following AMI. Then, the

Correspondence: Jun Li; Jie Wang
Guang'anmen Hospital, No. 5, Bixiange Road, Xicheng District, Beijing, China
Tel +86 010 8800 1817
Email gamyylj@163.com; jiewang1001@126.com

submit your manuscript | www.dovepress.com
Dovepress
http://dx.doi.org/10.2147/DDDT.S163405

myocardium gets thinner in the infarct zone, while myocardial hypertrophy gets more significant in the non-infarct zone. What is worse, contractile dysfunction, neurohormonal activation, histologic remodeling, inflammatory changes and apoptosis arise after AMI.[2] The gradual enlargement of the ventricular chamber caused by a series of physiologic and pathologic processes leads to hemodynamic changes, generating heart failure. Hence, VR following myocardial infarction (MI) is the significant pathologic basis of heart failure and is running through the whole process. Delaying or preventing VR is, therefore, critical factor for preventing heart failure.[3,4]

Paeoniflorin (PF) is the main active component of the commonly used Traditional Chinese Medicine peony, *Paeonia lactiflora* Pall. or *Paeonia veitchii* Lynch. PF has diverse biologic functions and inhibits platelet aggregation, thrombosis, atherosclerosis and tumor formation, dilates coronary vessels, increases coronary blood flow, improves microcirculation, protects the liver and so on.[5–12] Previous studies have also demonstrated that PF (10 mg/kg) reduced infarct size in ischemia/reperfusion injury rat, improved the hemodynamic parameters, decreased Caspase-3 and Bax expressions, but upregulated Bcl-2 in the left ventricles (LVs).[13] Recently, PF (5, 10, 20 mg/kg) has been shown to decrease the expression levels of tumor necrosis factor-α (TNF-α), interleukin (IL)-1β, IL-6 and nuclear factor-κB, inhibit the activities and protein expression levels of inducible nitric oxide synthase and repress Caspase-3 and Caspase-9 activities.[14] However, whether PF can ameliorate AMI and the potential underlying mechanisms in rats remains to be elucidated.

The cardioprotection of PF has been confirmed in the rats with MI during paracmasis by a pilot experiment in this test. Then, to further verify the curative effects and mechanisms of PF on the rats, the inflammatory factors, myocardial mitochondria and the expression of Caspase-3 and Caspase-9 were observed, indicating PF's effect on VR. We hypothesized that PF inhibited apoptosis, leading to increased myocardial salvage, reduced fibrosis size and mitigated VR in a rat model of AMI.

Materials and methods

Model establishment

A total of 120 male Wistar rats (SPF, 200±10 g) were purchased from Beijing Weitong Lihua Experimental Animal Co., Ltd. (SCXK 2015-0008). The research protocol was approved by the Animal Ethics Committee of Guang'anmen Hospital of China Academy of Chinese Medical Sciences (No. 2015EC035-02). The rats were kept in the animal room of Guang'anmen Hospital of China Academy of Chinese Medical Sciences, according to the Guide for the Care and Use of Laboratory Animals of the National Institutes of Health (Bethesda, MD, USA). The indoor temperature was maintained at 25°C±1°C. All rats had standard feed without eating and drinking restrictions.

The AMI model in rats was made by referring to the methods of references.[15,16] The specific procedures are as follows. The experimental rats were weighed and marked. After intraperitoneal injection of 10% chloral hydrate (0.33 g/kg; Sigma-Aldrich, St Louis, MO, USA) for anesthesia with skin preparation (shaving the hair), the rats were fixed in a supine position on a surgical table. Endotracheal intubation was conducted and fixed with lines after using iodophor for disinfection. The tracheal tube was connected with the HX-300 medical ventilator (Taimeng Technology Ltd., Chengdu, China), involving a tidal volume of 8 mL, frequency of 70 times/min and respiratory ratio of 1:3. An incision was made about 1 cm above the sternum slightly toward the left, and the muscular layer was separated bluntly. The thoracic cavity was opened with an eye speculum of ophthalmology by the third and fourth intercostal space to expose the heart and ligate the anterior descending coronary artery, while only threading was performed in rats selected randomly in the sham surgery group in advance, without ligation. Criteria of successful models are as follows: it was noted after ligation that the limb lead II significantly increased in the R wave amplitude, increased in the T wave and was markedly elevated in the ST segment, showing convexity and monophasic curve. Standard limb electrocardiogram indicated that the ST junction was markedly elevated. The color of the ligation site was grayish white. When the rats were stable, the thoracic skin was clamped with a hemostatic clamp and sutured carefully with removal of the medical ventilator. Subcutaneous injection of 100,000 IU penicillin was performed in each rat for preventing infection. After surgery, the rats were placed on the insulation blanket and covered with rugs to keep warm and increase the survival rate. The rats were observed closely all the time and chest compression for rescue was performed timely in the presence of ventricular fibrillation.

Animals in each group were given water and feed normally, and administered with medication since 2 hours after the recovering time. The AMI models of rats established successfully were gavaged for 28 days once daily.

Animal grouping and administration

One hundred and five of the 120 rats were made MI models and the remaining 15 had sham surgery. Among the 105 rats, 23 were excluded as 10 died, 9 had ventricular fibrillation and 4 models were unsuccessful. Therefore, the 82 rats that survived after surgery were randomly assigned to the model

group (18 rats), captopril group (16 rats) (4.50 mg/kg/d, No.1409021H, Sino-American Shanghai Squibb Pharmaceuticals Ltd., Shanghai, CHN), PF (No.110736-201337, National Institutes for Food and Drug Control, Beijing, CHN) groups with high dose, middle dose and small dose respectively (9.00, 4.50 and 2.25 mg/kg body weight [BW]/d, 16 rats in each group).[17] Rats in the sham surgery group and model group were administered with 10 mL/kg/d of 0.5% CMCC-Na solution. Also, other test substances were suspended in 0.5% CMCC-Na solution. Rats in the middle dose group were given the adult human equivalent dose of 70 kg (converted by the body surface area), while rats in the high-dose group were administered two times of adult human equivalent dose, and rats in the small-dose group were given one-half of the adult human equivalent dose.

Sampling and sample processing methods

After intraperitoneal injection of 10% chloral hydrate mixture (300 mg/kg), rats in each group were fixed on a dissecting table and their abdominal cavities were cut open. Blood of abdominal aorta was collected with a 10 mL syringe and treated on different indexes. Then, the thoracic cavities were cut after clamping the abdominal aorta using a hemostatic clamp. Next, the hearts were cut and lavaged quickly with ice-cold normal saline to wash the residual blood, and then water was blotted up using filter paper. Moreover, the whole hearts and LVs were set on the ice after weighing by an accurate electronic balance (Sartorius Scientific Instruments Co., Ltd., Beijing, China). Also, the apex of the heart of size 3×3 mm was selected and fixed with 3% glutaraldehyde for electron microscopy. Finally, the cardiac tissue at 0.3 cm under the ligature was fixed with 4% paraformaldehyde for HE staining and Masson staining. Peri-infarct tissue was defined as the area of myocardium within 2 mm of the visible edge of infarction, and remote area was taken from the interventricular septum,[18] while the rest of the tissues were immediately put into liquid nitrogen and stored in a refrigerator at −80°C.

Experimental methods for determining the effect to VR

The aim of this study was to observe the effect of PF on VR. Hence, the appearance, cardiac functions, left ventricle weight index (LVWI), myocardial cell morphology and other indexes reflecting VR were observed in the six groups of rats.

General observations

The appearance, activities, mental state, food intake, water intake, weight and stools were observed.

The BW and LVWI were weighed in rats with the electronic balance (Sartorius, BJ, CHN) in each group, respectively. Also, the LVWI (unit: mg/g) was calculated according to the following formula:

$$\text{LVWI} = \text{LV weight (mg)}/\text{BW (g)}$$

Cardiac function detection

After 28 days of gavage, the rats were anesthetized, and cardiac function was evaluated by Doppler ultrasonography. The BW was recorded and the heart rate, left ventricular ejection fraction (LVEF), left ventricular end-diastolic inner diameter (LVIDd), left ventricular end-systolic inner diameter (LVIDs) and other cardiac function parameters were measured by DW-350 B-mode echocardiography (Dawei Electronic Equipment Co. Ltd., Xuzhou, China).

Morphologic observations on VR

Morphological changes of myocardial cells in the infarct tissue were observed by HE staining, referring to the production methods of Zhang et al.[15] The degree of myocardial fibrosis in the infarct tissue was observed by Masson staining according to the methods of Itter et al.[16] In all experimental groups, the total amounts of fibrotic tissue (blue color) and muscle tissue (red tone) were determined in a standardized set of 10 cross-sections, starting at the level of the papillary muscle and moving toward the apex every 300 μm. The percentage of fibrosis was calculated from the ratio of the green area over the total (red + blue) area. The production was completed under the assistance of the Pathology Department, Guang'anmen Hospital, China Academy of Chinese Medical Sciences. The mitochondrial ultramicrostructure in the infarct tissue was observed with the transmission electron microscope, assisted by the Peking University School.

Apoptosis observation by terminal deoxynucleotidyl transferase dUTP nick end labeling (TUNEL)

Apoptosis was observed by the TUNEL assay.[19] Tissue sections were observed under a confocal microscope, in which the normal Tunel, muscle cell nuclei were blue, while the apoptotic nuclei showed varying shades of brown. Each slice in the same area of the distribution of apoptotic cells was randomly selected out of five high-power fields. Then, the average number of apoptotic cells in each field was calculated as a percentage of the total cell number. Thereby, the apoptosis index (%) was generated.

Detection of brain natriuretic peptide (BNP), TNF-α, IL-6 and IL-10

Serum BNP, TNF-α, IL-6 and IL-10 in rats were detected using the standard kit (MultiSciences Biotech Co. Ltd, Hangzhou, China). The specific procedures were performed strictly in accordance with the instructions of the kit. The OD values of all orifices were measured at 450 nm (410 nm if coloring by ABTS) after zeroing as the blank control orifice on a detector for enzyme-linked immunosorbent assay.

Detection of Caspase-3 and Caspase-9 proteins in remote heart tissue by immunohistochemistry

On the basis of immunohistochemical procedures,[20] the positive criteria and methods of treatment were as follows: as the positive criterion, the cytoplasm of myocardial cells was observed, because it was the major expression site for Caspase-3 and Caspase-9. Its color showed out brown, including brownish yellow, brown and dark brown in sections. The expression levels were estimated by integrated OD of the positive cells. Integrated OD was the average cumulative OD of the positive staining area of each group determined by ImageJ software.

Detection of Caspase-3 and Caspase-9 proteins in remote heart tissue by Western blot

The procedure was as follows. Total proteins in myocardial tissues were extracted and prepared as 10% separation gel. Also, the protein samples were detected, sealed and incubated with the first and second antibodies (1:500; Sigma-Aldrich), respectively. Electrochemiluminescence (Upstate Technology LLC, NYC, NY, USA) was added into the surface of the membranous protein, and then film exposure was done, with developing for 2 minutes and fixing treatment. The images were scanned for preservation and analyzed with ImageJ software, with the gray-scale value digitized on each special band. The gray-scale value of the target protein divided by the gray-scale value of GAPDH was used to express the relative content of the target protein of the samples.

Statistical analysis

Professional statistical software SPSS 17.0 was adopted for statistical analysis of data. The experimental data were represented as mean±SD ($\bar{x}$±s), and normal distribution test was conducted on the data. For the data which met normal distribution and homogeneity of variance, analysis of variance test or Student's *t*-test was adopted. For the data which did not meet normal distribution, nonparametric test was adopted. $P<0.01$ meant very significant difference, while $P<0.05$ meant significant difference.

Experimental results and analysis

Analysis of the number of tested animals and general situation

After 28 days of gavage, all rats survived in the sham operation group, 3 rats died in the model group and 1 rat died in the remaining groups; therefore, 15 rats survived in each group. Severe arrhythmia, ventricular fibrillation, massive hemorrhage and post-surgical wound infection were the major causes of death for rats during the experiment. Accidie, epilation, emaciation, anorexia, loose stool and other symptoms were observed to some extent in each group during the treatment, except for the sham surgery group. Among the rats, the ones in the model group showed the most severe symptoms. They had generally poor condition, markedly reduced activities, impetuosity, decrease in food intake, water intake and tachypnea. However, in the rats of the treatment groups, this general situation had significantly improved. In addition, BW had reduced in the model group rats compared to that in those of the sham surgery group, but there was no statistical difference in all groups ($P>0.05$; Figure 1).

Observation on LVWI

LVWI had increased significantly in the model group than that in the sham surgery group ($P<0.01$). Further comparison of this index with that in the model group showed that the

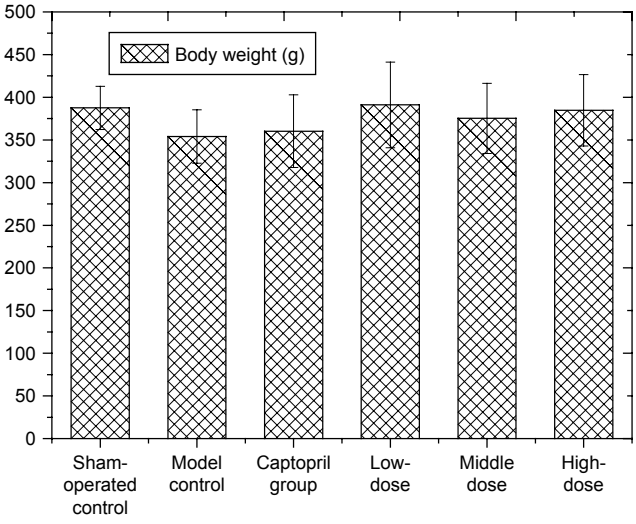

Figure 1 The body weight of rats ($\bar{x}$±s) (n=15/group).

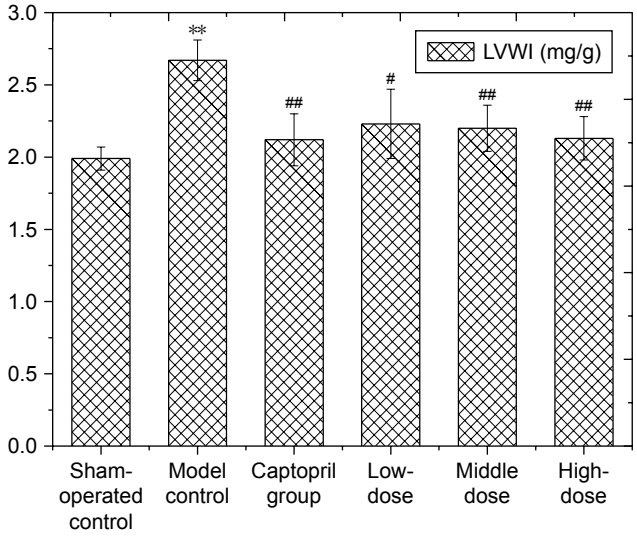

Figure 2 Effect of PF on LVWI in rats with myocardial infarction ($\bar{x}\pm s$).
Notes: $^{**}P<0.01$, n=15/group, versus sham-operated control; $^{\#}P<0.05$, $^{\#\#}P<0.01$, n=15/group, versus model control.
Abbreviations: LVWI, left ventricle weight index; PF, paeoniflorin.

captopril group and the PF group achieved reduced results (Figure 2).

Cardiac function

No statistically significant difference was observed in all parameters in all the groups before surgery ($P>0.05$). Twenty-eight days after surgery, there was no statistical difference in heart rate ($P>0.05$) (Figure 3A). While compared with that in the sham surgery group, the LVEF value decreased obviously in the model group ($P<0.01$), and significant enlargement was noted in LVIDd and LVIDs ($P<0.01$). Compared with the model group, the captopril group had higher LVEF value ($P<0.05$) and significantly improved LVIDd ($P<0.01$), but insignificant LVIDs change ($P>0.05$). The LVEF value was markedly higher in the PF group than that in the model group, with obvious reduction in LVIDd and LVIDs (Figure 3B–D).

Morphologic observation on VR

In the sham surgery group (Figure 4A), the myocardial cells showed no obvious degeneration and were arranged regularly and clearly. The myofilaments were relatively complete, and the intercellular space was even.

In the model group (Figure 4B), focal necrosis in the infarct tissue was identified in some myocardial cells, and the myocardial fibers dissolved and broke partly. A number of myocardial fibers showed obvious disorder in the arrangement. Karyopyknosis and karyorrhexis were noticed in several cells, and dilatation was seen in the myocardial capillaries. Further, more severe inflammatory cell infiltration and myocardial tissue necrosis were noted under the epicardium.

In the captopril group (Figure 4C), disordered arrangement was noted in local myocardial fibers, along with a small amount of myocardial cell degeneration, necrosis and slight inflammatory infiltration. A little capillary hyperemia was found (significantly slighter than that in the model group).

In the PF groups (Figure 4D–F), it could be seen that a small amount of myocardial cells were loose, edematous and necrotic. Compared with the model group, some myocardial fibers were arranged more regularly with slight inflammatory cell infiltration, and the overall morphology was relatively clear.

Masson staining

Results of Masson staining suggested that the myocardial cells were arranged very regularly in the sham surgery group (Figure 5A). No obvious hyperplasia was noticed in the collagen fibers of intercellular substances. But in the model group (Figure 5B), irregular arrangement was noted in the myocardial cells with more disordered structures in the infarct tissue. A large number of collagen fibers replaced the myocardial cells with obvious hypertrophy in some myocardial cells. Although collagen fibers were also observed to replace some myocardial cells and alternated with myocardial cells in the captopril group (Figure 5C) and PF groups (Figure 5D–F), the results were without significant statistical difference. This was, however, greatly reduced only in the PF-treated hearts. Quantification of the scar fraction (Figure 5G) confirmed that PF could significantly reduce fibrosis compared to the model group ($P<0.01$).

Results of mitochondrial ultramicrostructures

In the sham surgery group (Figure 6A), the ultramicrostructures of myocardial mitochondria were clear in rats, with more complete membranes, compact cristae, clear matrix, regular intercalated discs and favorable continuity, while there were several broad, broken or vacuolar mitochondrial cristae occasionally with disordered intercalated discs and unfavorable continuity.

In the model group (Figure 6B), the mitochondria showed obvious edema with broken cristae in some portions of the infarct tissue. Significantly increased collagen fibers were observed with more disordered arrangement and loose structures. The intimal and adventitial integrity was destroyed markedly and was even broken and dissolved with

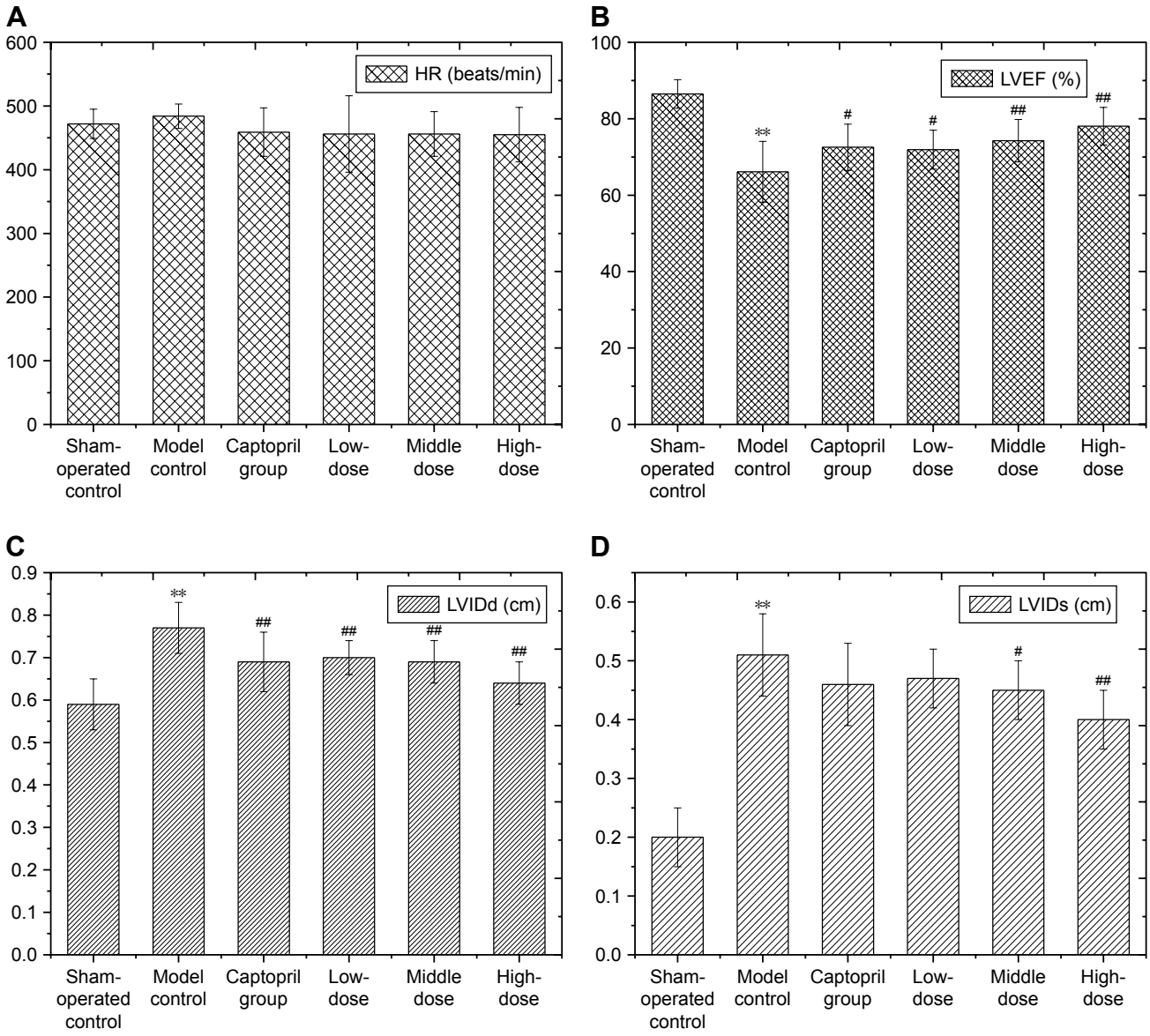

Figure 3 Effect of PF on cardiac function in rats with myocardial infarction ($\bar{x}\pm s$).
Note: (**A**) HR, (**B**) LVEF, (**C**) LVIDd and (**D**) LVIDs. $^{**}P<0.01$, n=15/group, versus sham-operated control, $^{\#}P<0.05$, $^{\#\#}P<0.01$, n=15/group, versus model control.
Abbreviations: HR, heart rate; LVEF, left ventricular ejection fraction; LVIDd, left ventricular end-diastolic inner diameter; LVIDs, left ventricular end-systolic inner diameter; PF, paeoniflorin.

overflowing content. Vague and disordered cristae were noted with some of them disappearing or vacuolating. The matrix was blurry with broken mitochondria. Uneven thickness existed in the myofibril with unclear structures of the sarcomere. Most of the myofilaments were destroyed and dissolved. Also, part of the disordered intercalated discs had poor continuity.

In the captopril group (Figure 6C), the myocardium cells were arranged more regularly. The arrangement of myofibrils was orderly, while some mitochondria were broken slightly and the sarcoplasmic reticulum expanded slightly. Furthermore, the myofilaments were arranged regularly and orderly, but some were broken.

In the PF groups (Figure 6D–F), the ultramicrostructure degeneration of myocardial cells was significantly reduced compared with that in the model group. Cristae of some mitochondria were slightly broken, and the myofilaments were arranged more regularly and some were loose or broken. Moreover, a little collagen hyperplasia was observed.

Results of apoptosis detected by TUNEL

Muscle cell nuclei were blue, but apoptotic nuclei were brown (Figure 7A–F) in remote heart tissue. Compared with the sham surgery group, apoptosis increased markedly in remote tissue in the model group ($P<0.01$). In comparison with the

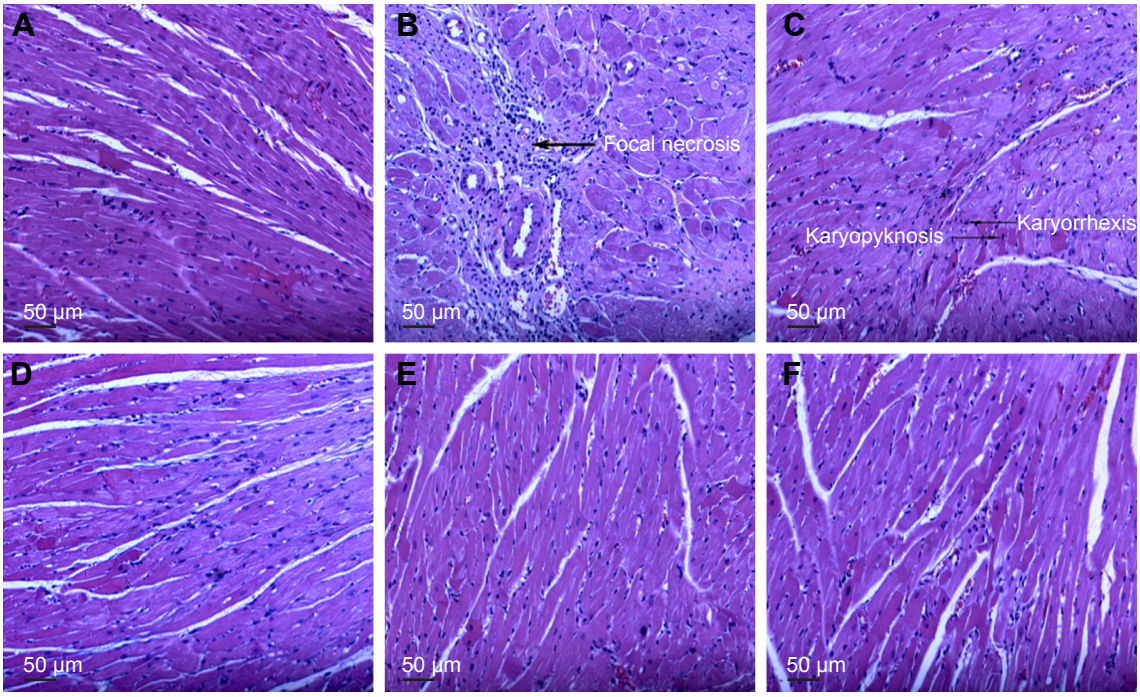

Figure 4 HE staining results.
Notes: Effect of PF on heart histopathology in rats with myocardial infarction (HE, ×200): (**A**) sham-operated control; (**B**) model control; (**C**) captopril group; (**D**) low-dose group; (**E**) middle dose group and (**F**) high-dose group.
Abbreviation: PF, paeoniflorin.

model group, apoptosis reduced obviously in the treatment groups ($P<0.01$; Figure 7G).

Results of BNP, TNF-α, IL-6 and IL-10

Compared with the sham surgery group, BNP increased markedly in the model group ($P<0.01$). However, BNP reduced markedly in the captopril group and PF groups, compared with that in the model group ($P<0.01$; Figure 8A). Compared with the sham surgery group, the concentrations of serum TNF-α and IL-6 increased markedly in the model group ($P<0.01$), while IL-10 reduced significantly ($P<0.01$). In contrast, TNF-α ($P<0.05$) and IL-6 ($P<0.01$) reduced obviously in the captopril group, whereas no statistical difference was noted in IL-10 ($P>0.05$) when compared to the model group. Similarly, TNF-α and IL-6 reduced markedly in the PF groups compared with those in the model group as well. More importantly, IL-10 was observed to increase significantly in the PF groups (Figure 8B–D).

Immunohistochemical results

Significant statistical differences were noted between the sham surgery group and other groups ($P<0.01$) in remote heart tissue. There were also obvious differences between the captopril group and PF groups compared with those in the model group ($P<0.01$). It was demonstrated that PF and captopril could markedly inhibit the expression of Caspase-3 and Caspase-9 proteins (Figures 9–11).

Western blot results

Compared with the sham surgery group, the expression levels of Caspase-3 and Caspase-9 proteins were increased significantly in the model group in remote heart tissue, while the expression of Caspase-3 and Caspase-9 proteins reduced markedly in the captopril group and the PF groups. Also, the treatment groups had lower expression than that in the model group. The results suggested that PF could significantly inhibit the expression of Caspase-3 and Caspase-9 proteins (Figures 12 and 13).

Discussion

LVEF evaluated by echocardiography was a more accurate measure of systolic function than ±dP/dt(max) in an MI model.[21] As revealed in this study, rats in the PF group generally improved with reduced LVWI and markedly increased LVEF, compared with those in the model group. Furthermore, the ventricular chambers reduced during systole and diastole, demonstrating that cardiac function in rats had been improved significantly by the treatment of PF. LV remodeling

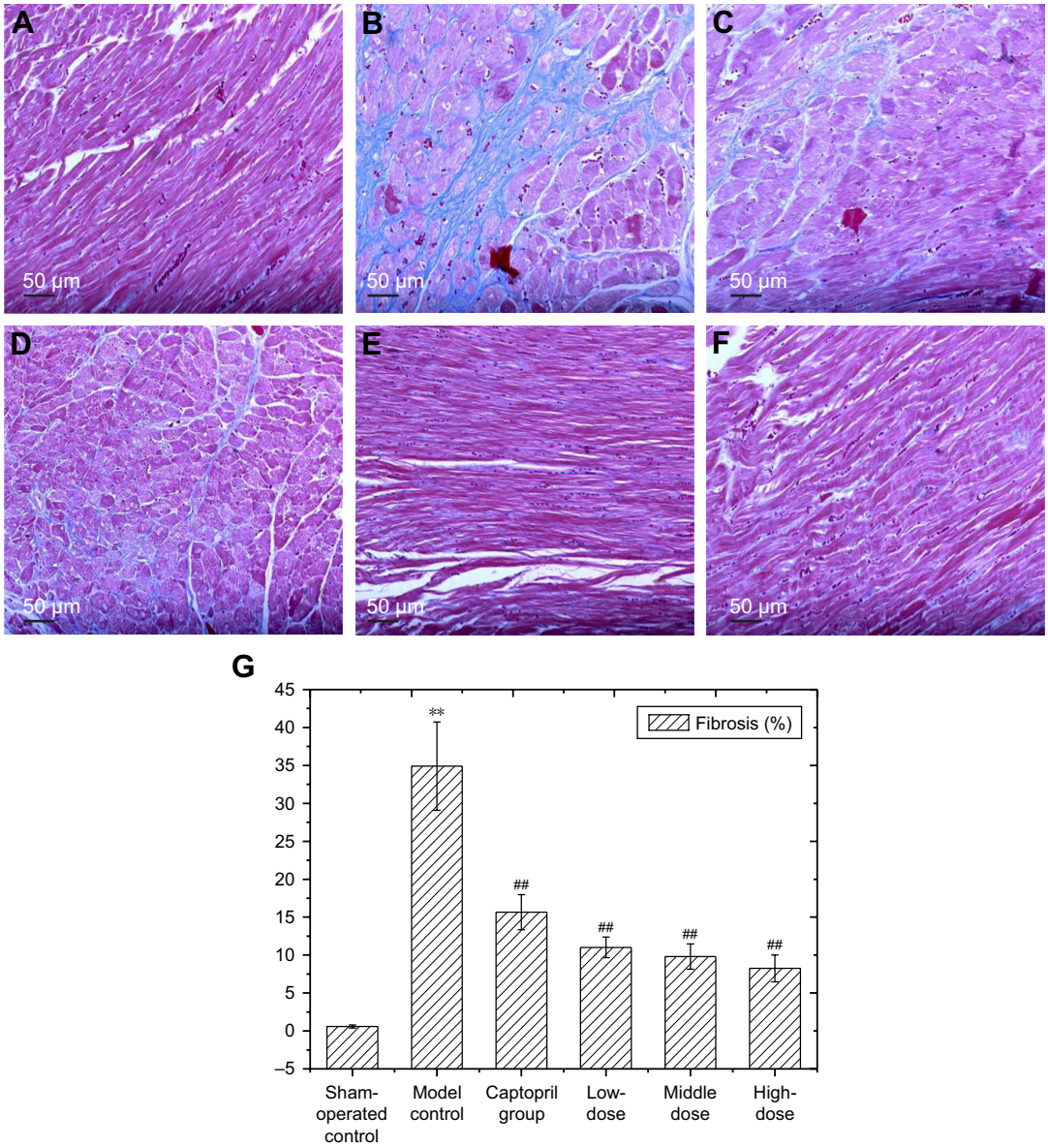

Figure 5 Effect of PF on heart histopathology in rats with myocardial infarction (Masson staining, ×200): (**A**) sham-operated control; (**B**) model control; (**C**) captopril group; (**D**) low-dose group; (**E**) middle dose group; (**F**) high-dose group and (**G**) fibrosis (%).
Notes: $^{**}P<0.01$, n=15/group, versus sham-operated control; $^{\#\#}P<0.01$, n=15/group, versus model control.
Abbreviation: PF, paeoniflorin.

was characterized by anatomic changes.[2] PF could improve these changes, and thereby inhibit LV remodeling. Further observation of myocardial tissues in the PF group by HE staining and Masson staining showed that the myocardial cells reduced in degeneration and were arranged regularly. In addition, the myofilaments were relatively complete, the space was relatively even, and the collagen fibers of intercellular substances obviously decreased. All the results suggested that the curative effects were equal to those in controls with positive drugs. By the treatment of PF, the structures of myocardial mitochondria in the rats improved markedly. The ultramicrostructures were clear with complete membrane, compact cristae, clear matrix, complete mitochondrial membranes and regularly arranged myofilaments.

Long-term activation of the neurohormonal response, especially of the sympathetic nervous system and the renin–angiotensin–aldosterone system, was a major molecular hallmark of adverse LV remodeling.[2] BNP in myocardial ischemia and hypoxia was synthesized, and its increased degree was positively correlated with the severity of myocardial ischemia and hypoxia.[22] In this study, BNP reduced markedly in the captopril group and the PF-treated groups.

Some researches have confirmed that the concentrations of TNF-α, IL-6 and IL-10 were closely associated

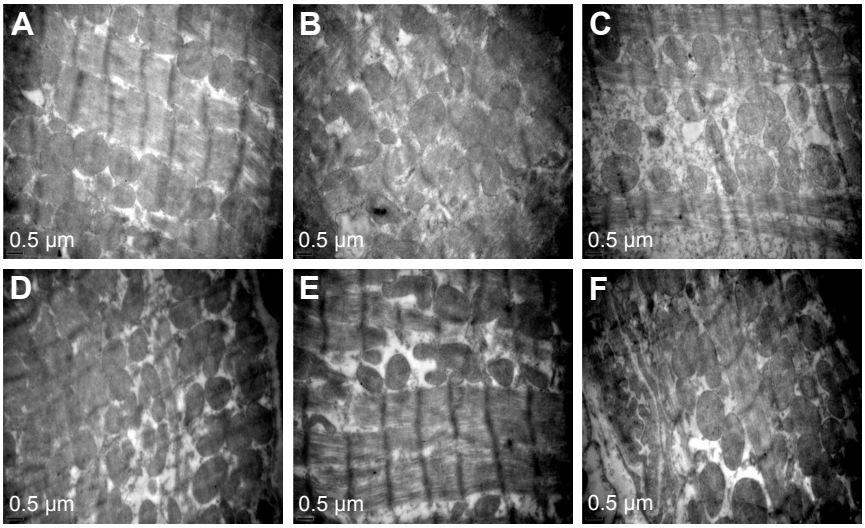

Figure 6 Effect of PF on myocardial mitochondria in rats with myocardial infarction (transmission electron microscope, ×20,000).
Note: (**A**) Sham-operated control; (**B**) model control; (**C**) captopril group; (**D**) low-dose group; (**E**) middle dose group and (**F**) high-dose group.
Abbreviation: PF, paeoniflorin.

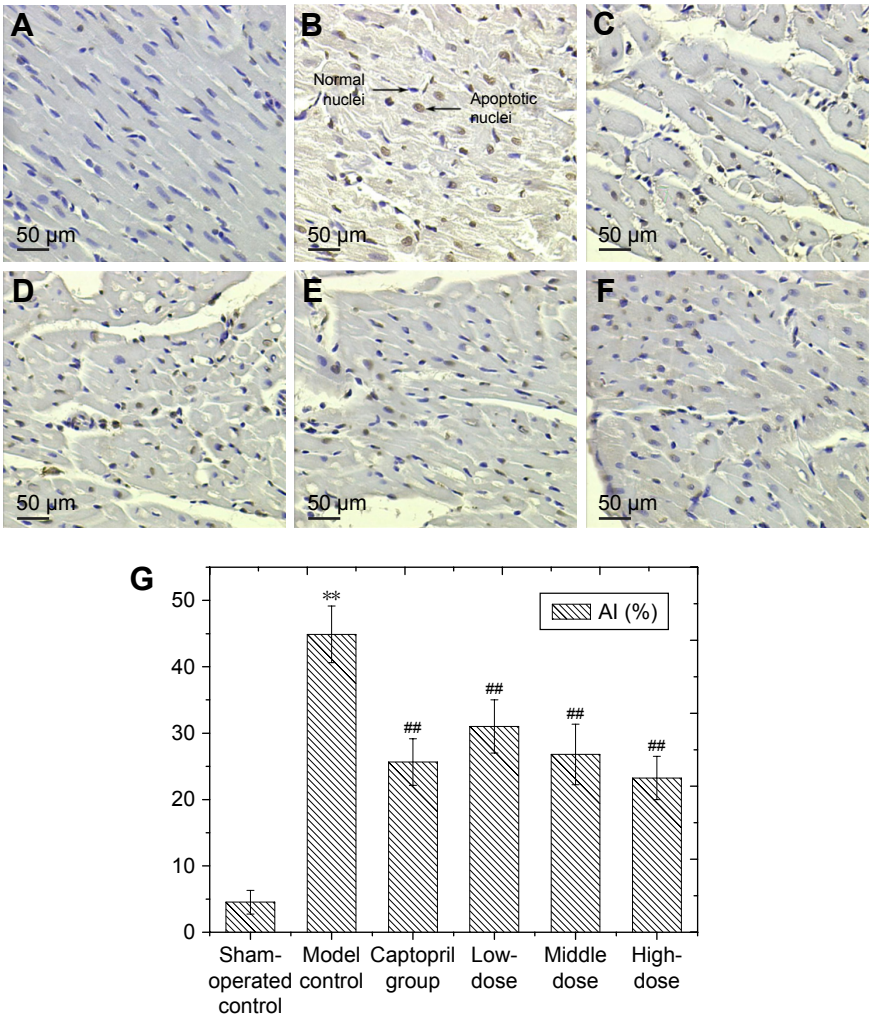

Figure 7 Effect of PF on apoptosis in rats with myocardial infarction ($\bar{x}\pm s$; TUNEL, ×200): (**A**) sham-operated control; (**B**) model control; (**C**) captopril group; (**D**) low-dose group; (**E**) middle dose group; (**F**) high-dose group and (**G**) AI (%).
Notes: $^{**}P<0.01$, n=15/group, versus sham-operated control; $^{\#\#}P<0.01$, n=15/group, versus model control.
Abbreviations: AI, apoptosis index; PF, paeoniflorin; TUNEL, terminal deoxynucleotidyl transferase dUTP nick end labeling.

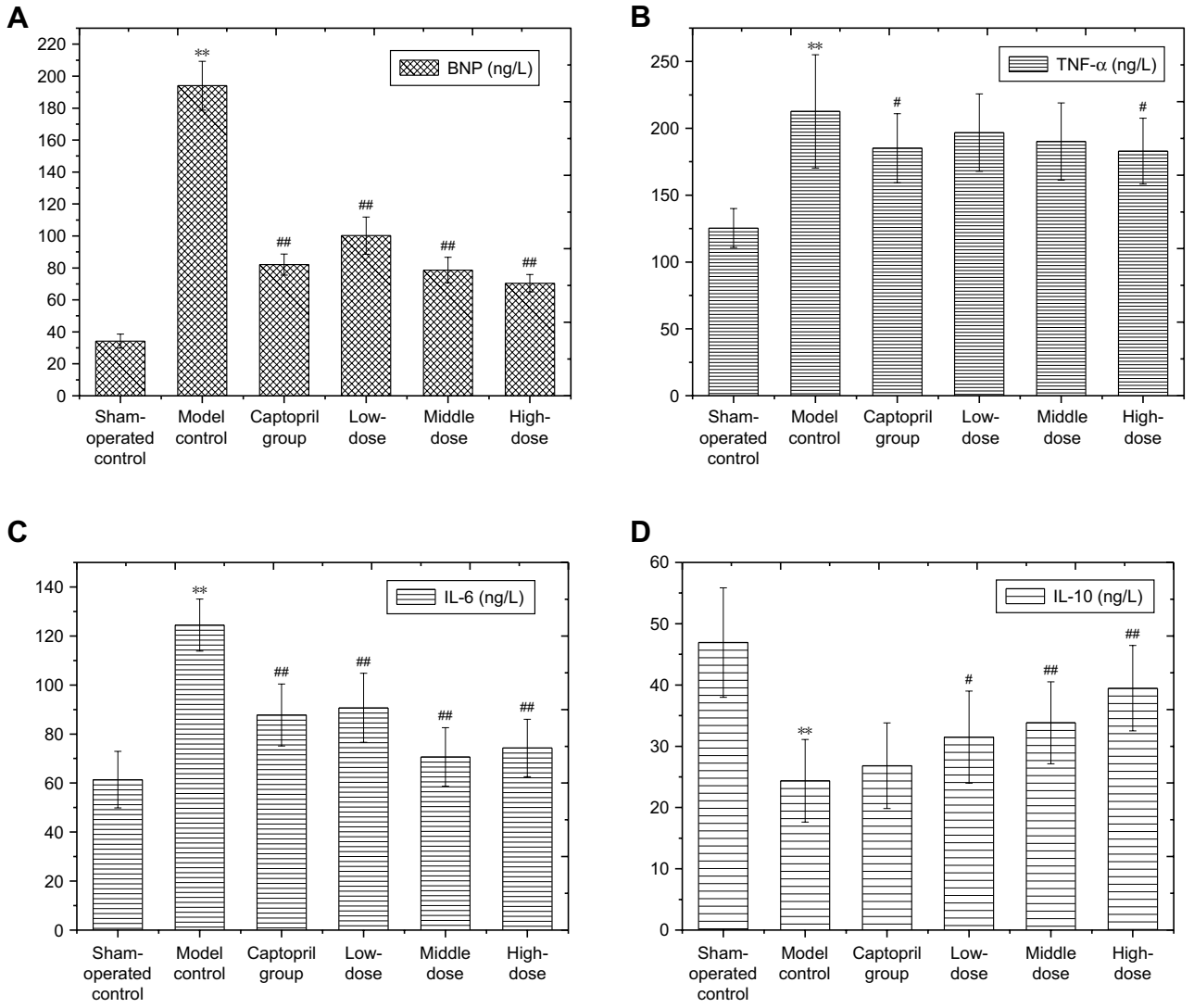

Figure 8 Effects of PF on the levels of BNP, TNF-α, IL-6 and IL-10 in rats with myocardial infarction ($\bar{x}\pm s$).
Note: (**A**) BNP, (**B**) TNF-α, (**C**) IL-6 and (**D**) IL-10; $^{**}P<0.01$, n=15/group, versus sham-operated control; $^{\#}P<0.05$, $^{\#\#}P<0.01$, n=15/group, versus model control.
Abbreviations: BNP, brain natriuretic peptide; IL-6, interleukin-6; IL-10, interleukin-10; PF, paeoniflorin; TNF-α, tumor necrosis factor-α.

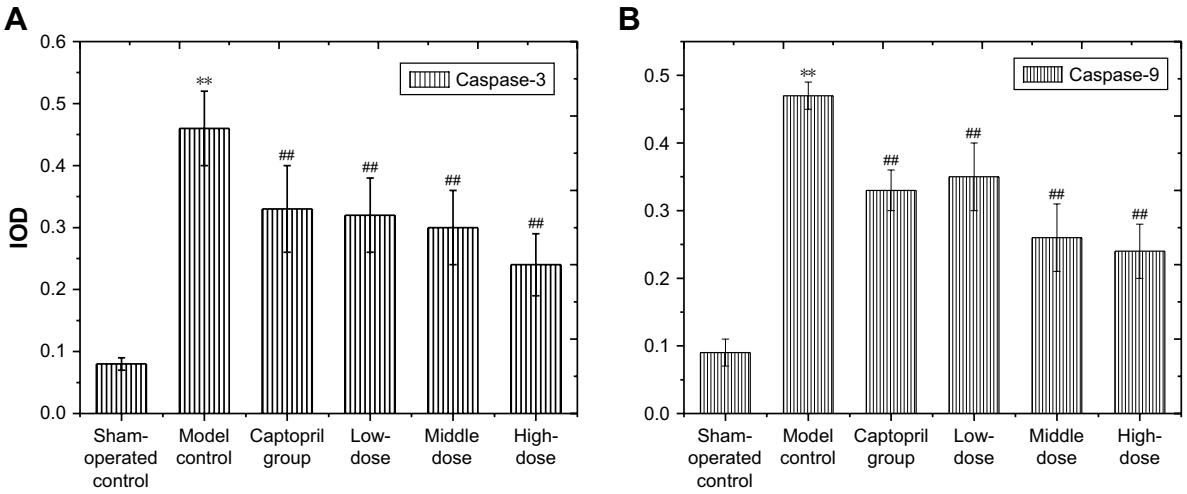

Figure 9 Effects of the PF on the expression of Caspase-3 and Caspase-9 (IOD) in rats with myocardial infarction ($\bar{x}\pm s$).
Notes: (**A**) Caspase-3, (**B**) Caspase-9. $^{**}P<0.01$, n=15/group, versus sham-operated control, $^{\#\#}P<0.01$, n=15/group, versus model control.
Abbreviations: IOD, integrated optical density; PF, paeoniflorin.

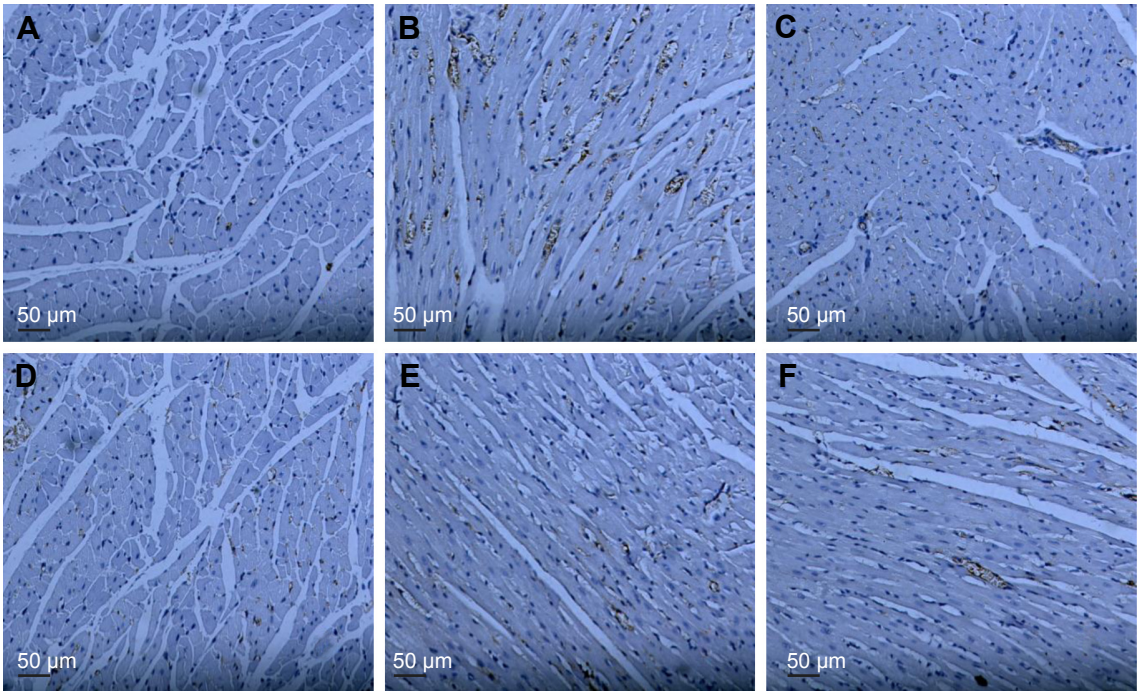

Figure 10 Expression of PF on the expression of Caspase-3 in myocardial cells by immunohistochemistry (inverted microscope, ×200).
Note: (**A**) Sham-operated control, (**B**) model control, (**C**) captopril group, (**D**) low-dose group, (**E**) middle dose group and (**F**) high-dose group.
Abbreviation: PF, paeoniflorin.

with the severity of heart failure.[23] TNF-α promoted VR after MI by initiating a cascade reaction of inflammatory cells. During VR, the interaction of IL-6 and its receptors could gradually induce cardiac fibroblasts to transform into myofibroblasts. Moreover, it promoted a large amount of collagen protein secretion by stimulating mature fibroblasts in the heart, and precipitated cardiac fibrosis and myocardial cell growth.[23] IL-10 could effectively prevent

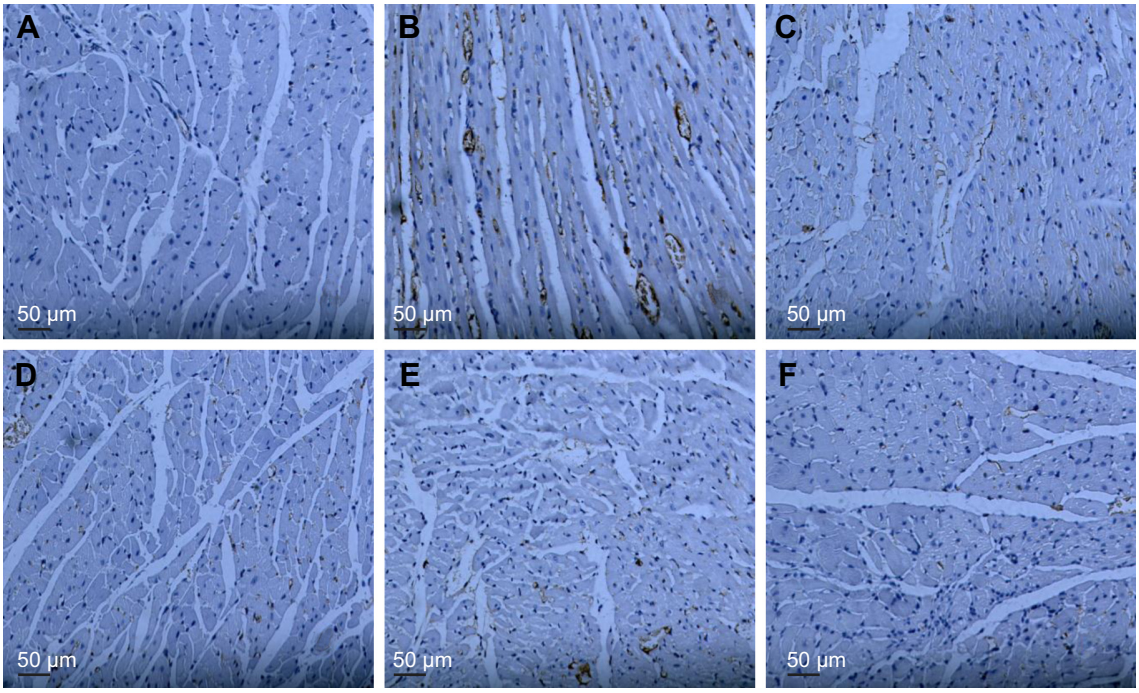

Figure 11 Effect of the PF on the expression of Caspase-9 in rats with myocardial infarction (immunohistochemistry, ×200).
Note: (**A**) Sham-operated control, (**B**) model control, (**C**) captopril group, (**D**) low-dose group, (**E**) middle dose group and (**F**) high-dose group.
Abbreviation: PF, paeoniflorin.

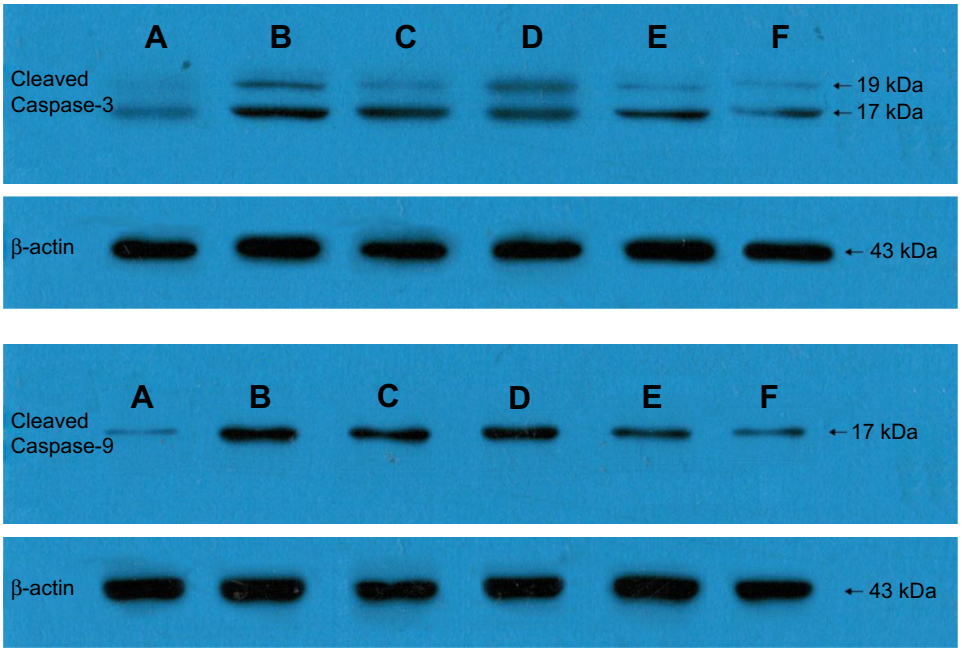

Figure 12 Effect of the PF on the expression of Caspase-3 and Caspase-9 in rats with myocardial infarction (Western blot).
Note: (**A**) Sham-operated control, (**B**) model control, (**C**) captopril group, (**D**) low-dose group, (**E**) middle dose group and (**F**) high-dose group.
Abbreviation: PF, paeoniflorin.

the proliferation and activation of inflammatory cells, and thus improve VR. In general, inflammatory cytokines, such as IL-10, could affect the results from two aspects: on the one hand, they could inhibit the inflammatory reaction and protect the heart, helping in gradually recovering from the heart injury, and thus playing a positive role. On the other hand, they played a negative role and could stimulate and aggravate the inflammation, resulting in aggravation of the heart injury and causing further heart failure. In this study, in comparison with the sham surgery group and the model group, significant differences were noted in inflammatory factors such as TNF-α, IL-6 and IL-10. These results suggested that there were inflammatory mechanisms in the MI model caused by ligation of coronary arteries. On the contrary, obvious changes were noticed in the inflammatory cytokines after treatments. Captopril could downregulate the concentration of serum TNF-α and IL-6, but without obvious regulation in IL-10. PF, however, could downregulate serum

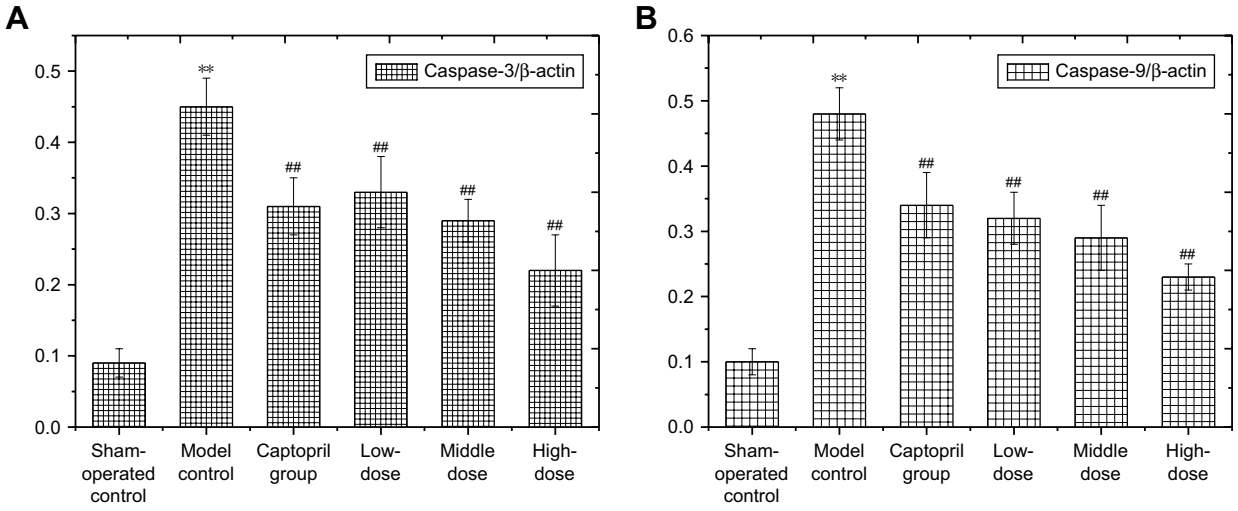

Figure 13 Effects of PF on the expression of Caspase-3 and Caspase-9 in rats with myocardial infarction ($\bar{x}\pm s$): (**A**) Caspase-3/β-actin; (**B**) Caspase-9/β-actin.
Note: $^{**}P<0.01$, n=15/group, versus sham-operated control, $^{\#\#}P<0.01$, n=15/group, versus model control.
Abbreviation: PF, paeoniflorin.

TNF-α and IL-6 and upregulate IL-10, showing two-way comprehensive action. It, therefore, demonstrated that one of the mechanisms against VR by PF was the regulation of inflammatory factors with a comprehensive, all-round and favorable two-way method. PF improved and slowed down the effects of the inflammatory cascade reaction during VR, and held back the continuous development of VR, thus preventing heart failure.

Current researches on heart failure were focused on the mechanism of energy metabolism dysfunction, as this disorder of myocardia was one of the leading causes of the occurrence and development of heart failure. The mitochondrial structure was destroyed during congestive heart failure (CHF) in which adenosine triphosphate formation decreased, energy supply became insufficient and myocardial apoptosis was promoted. In addition, myocardial apoptosis was demonstrated to be the major mechanism of myocardial remodeling in CHF. Therefore, determining the mechanism of mitochondrial energy metabolism dysfunction may provide new therapeutic targets and strategies for the treatment of heart failure.[24,25] In chronic heart failure rats, and model rabbits with heart failure induced by volume overload and myocardial ischemia and reperfusion, as revealed in the studies, Caspase-3 and Caspase-9 were involved in the pressure load-induced heart failure and in the occurrence and development of myocardial remodeling. Further, the concentrations of the two factors were positively correlated with severity of heart failure.[20,26] Hence, we speculated that Caspase-3 and Caspase-9 participated in myocardial apoptosis in rats with heart failure following myocardial infarction.

Research revealed that myocardial apoptosis was involved in the whole process of heart failure.[27] Myocardial apoptosis appeared immediately since heart failure, which may be closely associated with a significant increase in intraventricular pressure and the excessive activation of local intracardiac renin-angiotensin system. Apoptosis, which is active cell death regulated by genes, was characterized by the initiation of apoptotic signaling pathways and expression of relevant genes. Caspase-3 is an important protease during apoptosis and also a marker enzyme of apoptosis.[28] Myocardial apoptosis activated the caspases family via the death receptor pathway or mitochondrial pathways.[29] Caspase-9 was activated by apoptotic bodies, promoted by various proapoptotic factors during the process of apoptosis, which promoted the expression of Caspase-3 in the downstream caspase family. Caspase-3 was finally required to perform the process of myocardial apoptosis.[30] It has been demonstrated in this study that PF could downregulate the expression of Caspase-3 and Caspase-9 in rats with heart failure. Also, the intervention could markedly improve clinical symptoms and cardiac function indexes in heart failure rats, showing significant differences compared with those in the model group. Hence, it was speculated that PF could reduce cell apoptosis, inhibit VR, and improve or delay the formation and development of heart failure. These, therefore, may be the mechanisms for treatment for heart failure following MI.

Conclusion

The PF could significantly improve the cardiac function in rats with VR after AMI. It also adjusted the inflammatory cytokines of TNF-α, IL-6 and IL-10. Furthermore, it reduced the BNP level and inhibited the expression of Caspase-3 and Caspase-9. This study has provided a preliminary discussion on the treatment mechanism of PF for CHF from the viewpoint of disease, whereas curative effects based on disease-syndrome animal model, expression of other cytokines and molecular mechanisms are still worth continuing in this research.

Acknowledgments

This study was supported by National Major Scientific and Technological Special Project for "Significant New Drugs Development" (No. 2013ZX09301307) and the National Natural Science Foundation of China (No. 81503421).

Author contributions

All authors contributed toward data analysis, drafting and revising the paper and agree to be accountable for all aspects of the work.

Disclosure

The authors report no conflicts of interest in this work.

References

1. Santos-Gallego CG, Picatoste B, Badimón JJ. Pathophysiology of acute coronary syndrome. *Curr Atheroscler Rep*. 2014;16(4):401.
2. Santosgallego CG, Vahl TP, Goliasch G, et al. Sphingosine-1-phosphate receptor agonist fingolimod increases myocardial salvage and decreases adverse postinfarction left ventricular remodeling in a porcine model of ischemia/reperfusion. *Circulation*. 2016;133:954–966.
3. Macintyre L, Capewell S, Stewart S, et al. Evidence of improving prognosis in heart failure: trends in case fatality in 66547 patients hospitalized between 1986 and 1995. *Circulation*. 2000;102(10):1126–1131.
4. Motiwala SR, Gaggin HK. Biomarkers to predict reverse remodeling and myocardial recovery in heart failure. *Curr Heart Fail Rep*. 2016;13(5):207–218.
5. Wang W, Zhang Y, Liu C, Meng C, Wang BM. Effects of Paeoniforin on the cholinergic anti-inflammatory pathway and related factors. *Chin J Tradit Chin Med Pharm*. 2016;31(3):1106–1108.

6. Chen T, Guo ZP, Jiao XY, et al. Peoniflorin suppresses tumor necrosis factor-α induced chemokine production in human dermal microvascular endothelial cells by blocking nuclear factor-κB and ERK pathway. *Arch Dermatol Res*. 2011;303(5):351–360.
7. Wang YK, Huang ZQ. Effect on angiotenstin II-induced rat arterial smooth muscle cell proliferation of paeoniflorin. *J Emergency Tradit Chin Med*. 2012;21(3):399–400, 516.
8. Jin SN, Wen JF, Wang TT, Kang DG, Lee HS, Cho KW. Vasodilatory effects of ethanol extract of *Radix Paeoniae Rubra* and its mechanism of action in the rat aorta. *J Ethnopharmacol*. 2012;142(1):188–193.
9. Ji QL, Yang LN, Zhou J, et al. Protective effects of paeoniflorin against cobalt chloride-induced apoptosis of endothelial cells via HIF-1α pathway. *Toxicol in Vitro*. 2012;26(3):455–461.
10. Lin HR. Paeoniflorin acts as a liver X receptor agonist. *J Asian Nat Prod Res*. 2013;15(1):35–45.
11. Mo X, Zhao N, Du X, Bai L, Liu J. The protective effect of peony extract on acute myocardial infarction in rats. *Phytomedicine*. 2011; 18(6):451–457.
12. Rao ML, Tang M, He JY, Dong Z. Effects of paeoniflorin on cerebral blood flow and the balance of PGI_2/TXA_2 of rats with focal cerebral ischemia-reperfusion injury. *Acta Pharm Sinica*. 2014;49(1): 55–60.
13. Nizamutdinova IT, Jin YC, Kim JS, et al. Paeonol and paeoniflorin, the main active principles of *Paeonia albiflora*, protect the heart from myocardial ischemia/reperfusion injury in rats. *Planta Med*. 2008; 74(1):14–18.
14. Chen C, Du P, Wang JJ. Paeoniflorin ameliorates acute myocardial infarction of rats by inhibiting inflammation and inducible nitric oxide synthase signaling pathways. *Mol Med Rep*. 2015;12(3):3937–3943.
15. Zhang DY, Luo YH, Yang H, Tan S, Li FQ. Comparison between experimental models of chronic heart failure established by coronary artery ligature and abdominal aorta constriction. *J Chin Microcirc*. 2005; 9(3):171–174.
16. Itter G, Jung W, Juretschke P, Schoelkens BA, Linz W. A model of chronic heart failure in spontaneous hypertensive rats (SHR). *Lab Anim*. 2004;38(2):138–148.
17. Wei W, Wu XM, Li YJ. *Methodology of Pharmacological Experiment*. 4th edition. Beijing: People's Medical Publishing House, 2010.
18. Kido M, Du L, Sullivan CC, et al. Hypoxia-inducible factor 1-alpha reduces infarction and attenuates progression of cardiac dysfunction after myocardial infarction in the mouse. *J Am Coll Cardiol*. 2005; 46(11):2116–2124.
19. Melly L, Cerino G, Frobert A, et al. Myocardial infarction stabilization by cell-based expression of controlled Vascular Endothelial Growth Factor levels. *J Cell Mol Med*. 2018;22(3):1–12.
20. Yang B, Ye D, Wang Y. Caspase-3 as a therapeutic target for heart failure. *Expert Opin Ther Targets*. 2013;17(3):255–263.
21. Ishikawa K, Chemaly ER, Tilemann L, et al. Assessing left ventricular systolic dysfunction after myocardial infarction: are ejection fraction and dP/dt(max) complementary or redundant? *Am J Physiol Heart Circ Physiol*. 2012;302(7):H1423–H1428.
22. de Lemos JA, Mcguire DK, Drazner MH. B-type natriuretic peptide in cardiovascular disease. *Lancet*. 2003;362(9380):316–322.
23. Haugen E, Gan LM, Isic A, Skommevik T, Fu M. Increased interleukin-6 but not tumour necrosis factor-α predicts mortality in the population of elderly heart failure patients. *Exp Clin Cardiol*. 2008;13(1):19–24.
24. Di Lisa F, Canton M, Menabo R, Kaludercic N, Bernardi P. Mitochondria and cardioprotection. *Heart Fail Rev*. 2007;12(3–4):249–260.
25. Ashrafian H, Frenneaux MP. Metabolic modulation in heart failure: the coming of age. *Cardiovasc Drugs Ther*. 2007;21(1):5–7.
26. Samali A, O'Mahoney M, Reeve J, et al. Identification of an inhibitor of caspase activation from heart extracts; ATP blocks apoptosome formation. *Apoptosis*. 2007;12(3):465–474.
27. Kang PM, Izumo S. Apoptosis in heart: basic mechanisms and implications in cardiovascular diseases. *Trends Mol Med*. 2003;9(4): 177–182.
28. Higuchi M, Aggarwal BB, Yeh ET. Activation of CPP32-like protease in tumor necrosis factor-induced apoptosis is dependent on mitochondrial function. *J Clin Invest*. 1997;99(7):1751–1758.
29. Prabhu SD, Wang GW, Luo JZ, Gu Y, Ping PP, Chandrasekar B. Beta-Adrenergic receptor blockade modulates Bcl-X(S) expression and reduces apoptosis in failing myocardium. *Mol Cell Cordial*. 2003; 35(5):483–493.
30. Herbeuval JP, Lambert C, Sabido O, et al. Macrophages from cancer patients: analysis of TRAIL, TRAIL receptors, and colon tumor cell apoptosis. *J Natl Cancer Inst*. 2003;95(8):611–621.